water

MDPI

Article

Investigation on the Cavity Backwater of Chute Aerators under Various Atmospheric Pressures

Yameng Wang, Jun Deng and Wangru Wei *

State Key Laboratory of Hydraulics and Mountain River Engineering, Sichuan University, Chengdu 610065, China; wangyameng@stu.scu.edu.cn (Y.W.); djhao2002@scu.edu.cn (J.D.)
* Correspondence: weiwangru@scu.edu.cn

Abstract: A chute aerator is a device that entrains air into water and protects against cavitation erosion. The state of the jet cavity determines the aerator efficiency under different flow conditions. In the case of a low Froude number and low velocity, backwater is generated in the jet cavity. In severe cases, this backwater blocks the air intake holes and affects air intake efficiency. With the development and construction of water conservancy projects, an increasing number of dams have been constructed at altitudes above 3000 m. The influence of cavity backwater depth at reduced atmospheric pressures is unknown and may increase the risk of high-speed aerated flows in high-altitude areas. In this study, the relevant parameters of backwater were measured at various atmospheric pressures, including the jet length, cavity subpressure, backwater depth, and net cavity length. The pressure difference of atmospheric pressure can range from 0 to 94 kPa. The test results indicate that a decrease in atmospheric pressure causes variations in the cavity subpressure. The absolute value of the difference between the inside and outside of the cavity decreases with a decrease in atmospheric pressure. An empirical formula for calculating the subpressure at different atmospheric pressures is proposed for $P_N < 0.1$. The air velocity in the ventilation shaft decreases with a decrease in atmospheric pressure. The effects of variation in the atmospheric pressure on jet length can be ignored because the variation in jet length with different atmospheric pressures was constant. Additionally, the influence of varying atmospheric pressure on the cavity backwater is evident. The backwater depth decreases with a decrease in atmospheric pressure. When the atmospheric pressure decreases from 96 to 6 kPa, the maximum reduction in backwater depth is over 50%. Atmospheric pressure is a parameter that affects cavity backwater. Based on the measured backwater depth data, an empirical formula for calculating the backwater depth at different atmospheric pressures is proposed. This indicates a relationship between the atmospheric pressure and backwater depth under different flow conditions. It was further found that the bottom cavity may require a larger air intake volume at low atmospheric pressures and that it is necessary to optimize the aerator and the ventilation system.

Keywords: atmospheric pressure; backwater depth; cavity subpressure; jet cavity; aeration

Citation: Wang, Y.; Deng, J.; Wei, W. Investigation on the Cavity Backwater of Chute Aerators under Various Atmospheric Pressures. *Water* **2022**, *14*, 1513. https://doi.org/10.3390/w14091513

Academic Editors: Chang Lin and James Yang

Received: 1 March 2022
Accepted: 6 May 2022
Published: 9 May 2022

1. Introduction

Since 1897, severe cavitation damage to wall surfaces around high-velocity flows has been observed [1–4]. Since then, measures to prevent cavitation damage under high-velocity flow conditions have been proposed and studied. Aerating water is an effective measure for preventing cavitation damage. Aeration is often used in engineering and has the advantages of simple implementation and low cost. Therefore, modern spillways are often equipped with aeration steps to avoid cavitation damage [5,6]. With the development of water-air two-phase flow research, the cavitation damage situation has improved. However, with the development of water resources in China, an increasing number of dams have been constructed at altitudes of 3000 m or higher. The higher the altitude, the lower the atmospheric pressure. This creates a new problem because lower atmospheric pressure can affect the characteristics of aeration. For example, the elevation of

the Lianghekou Hydropower Station is approximately 2865.0 m. Compared to the typical pressure (P_0 = 96 kPa), the atmospheric pressure at the Lianghekou Dam is lower by 32.9%. The elevation of the Jiacha Hydropower Station is approximately 3000.0 m, and the atmospheric pressure at this location is approximately 65.8% of the typical pressure. Air intake and cavity characteristics are affected by varying atmospheric pressures. Currently, most model tests are conducted under normal atmospheric pressure without considering the difference between the altitude of the actual project and the altitude of the model location. Reduced atmospheric pressure influences cavity backwater, jet length, and air entrainment capacity, thus posing a significant threat to flood discharge safety. However, research in this area is limited.

Chanson and Kramer et al. [7–10] described streamwise air transport partially along the far-field flow zone downstream of chute aerators and measured the performance of the aerators for varying discharges, heads, and gate openings under varying cavity subpressures. The efficiency of an aerator is closely related to its shape design parameters, and one of the most important parameters is the jet length. The jet length is an important factor for measuring the cavity state. A longer bottom cavity is beneficial for increasing aeration in the water flow. Water flows through the aerator to form a jet, which forms a cavity under the water tongue and then drops to the bottom plate to flow downwards. There are many calculation methods for the bottom jet length, and the calculation of jet length mainly adopts the jet method, dimensional analysis, and numerical simulation [11–15]. Wu [16] considered the influence of the emergence angle on the jet trajectory, established a calculation method for the emergence angle, and improved the calculation accuracy of the bottom jet length. However, these methods did not consider the possibility of backwater in the bottom cavity. Currently, there is no high precision method for calculating backwater in the bottom cavity. Yang [17] studied the aeration characteristics of an aerator in a low-Froude-number flow, analyzed the problem of backwater in the cavity, and established a cavity backwater equation according to the momentum balance. Based on Yang's results, Xu [18] optimized the control body of the cavity backwater and improved the calculation formula for calculating the depth of the cavity backwater and net cavity length, thereby improving the calculation accuracy. The results revealed that the backwater height decreased with an increase in the Froude number. This research was of great significance for the calculation of backwaters under normal atmospheric pressure. Although the influence of cavity subpressure on backwater was considered in their analysis, varying atmospheric pressures were not considered, and some assumptions and calculations were still unreasonable.

To prevent cavitation damage in a flood spillway, the aeration concentration in the water flow must reach a certain degree, which requires jet flow through the aerator to form a good flow pattern and sufficient cavity space for aeration. Most previous research results on the bottom cavity ignored varying atmospheric pressures and assumed a normal atmospheric pressure. Some decompression models have been conducted to study changes in the jet length, cavity subpressure, and backwater in the bottom cavity under various atmospheric pressure conditions. The analysis of this type of data typically focused on changes in the backwater in the bottom cavity.

2. Hydraulic Model

Experiments were conducted in a 0.3-m-wide, 6-m-long sectional chute model at the State Key Laboratory of Hydraulics and Mountain River Engineering, Sichuan University, China (Figure 1). The model consisted of an upstream chute, aeration step, and downstream chute. The test model was constructed using plexiglass. The experimental model was placed in a pressure-reducing tank, which is a device that can adjust the atmospheric pressure. The aerator height was d = 5 cm, there were air holes on both sides of the aeration step, and the size of the air holes was 3 × 5 cm. The downstream chute slope was $i = \tan \alpha = 0.12$. The approach flow velocity V_0 and Froude number $F_0 = V_0/(gh)^{0.5}$ were generated with a jet cavity, where V_0 was the approach flow velocity, h was the approach flow

depth, and g was the gravitational acceleration. The atmospheric pressure in the pressure-reducing tank varied from 6 to 96 kPa, and the maximum vacuum degree reached 97%. The term "vacuum" refers to the rarity of gas, and $\eta_m = (P_0 - P_a)/P_0$, where P_0 represents the atmospheric pressure outside the pressure-reducing tank and P_a represents the atmospheric pressure inside the pressure-reducing tank. The cavity subpressure is expressed as $\Delta P = P_a - P_c = \rho g h_s$, $P_N = \Delta P/\rho g h$, where P_N is known as the cavity subpressure index, P_c represents the atmospheric pressure in the bottom cavity, and h_s represents the cavity subpressure head. The h_s values in the bottom cavity were determined using a U-shaped piezometer to the nearest millimeter, and h_s represents the difference between atmospheric pressure and bottom cavity pressure. The backwater depth was represented by y_0, which refers to the vertical distance from point B to the x-axis (Figure 1).

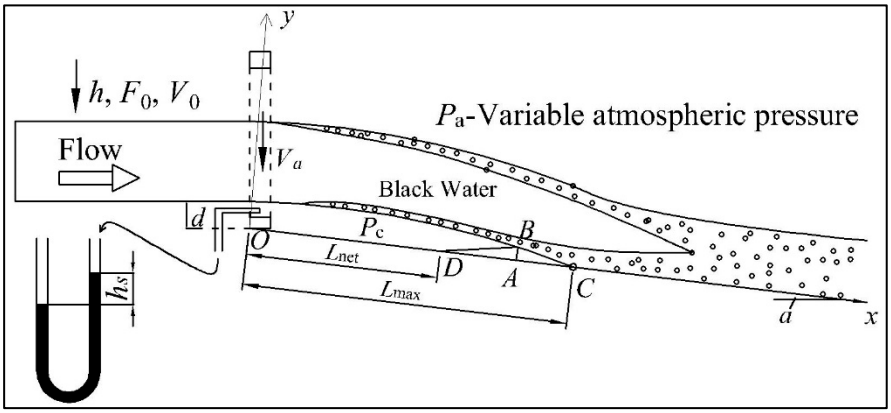

Figure 1. Definition scheme with the model.

The backwater in the bottom cavity fluctuates, and the influence of the fluctuation of the backwater in the cavity was ignored by assuming that it was a static water body. The atmospheric pressure was varied in steps of 10 kPa and the samples were divided into 10 groups. The Froude Number of the approach flow was adjusted on different atmospheric pressure conditions, and the Froude number ranged from $2.81 \leq F_0 \leq 8.92$, $2.0 \times 10^5 < Re < 6.1 \times 10^5$. $Re = (V_0\, h)/v$, where v = kinematic water viscosity. The contour line $C = 0.9$ was considered the water surface line at the lower edge of the water tongue, and the jet length (L) was determined through concentration measurements and observations. The flow direction starting from the edge of the aerator along the bottom of the downstream was the x-axis, and the vertical direction was the y-axis. In this study, the cavity subpressure, jet length, and cavity backwater were measured using different approaches based on the Froude number and decreasing atmospheric pressure. An airflow monitor (Fluke 922 Micromanometer) was used to measure the air velocity V_a in the shaft. The water velocity was measured by a CQY-SCU-FZ1.0 aeration current meter (Chengdu, China). The test conditions of the different series, including different hydraulic conditions, are listed in Table 1.

Table 1. Test program and parameter.

Series	F_0	h [m]	i	d [m]	Re	P_a [kPa]
S1	3.28	0.1	0.12	0.05	3.2×10^5	96~6
S2	3.76	0.1	0.12	0.05	3.7×10^5	96~6
S3	4.21	0.1	0.12	0.05	4.1×10^5	96~6

Table 1. *Cont.*

Series	F_0	h [m]	i	d [m]	Re	P_a [kPa]
S4	4.71	0.1	0.12	0.05	4.6×10^5	96~6
S5	4.96	0.1	0.12	0.05	4.9×10^5	96~6
S6	5.10	0.1	0.12	0.05	5.0×10^5	96~6
S7	5.57	0.1	0.12	0.05	5.5×10^5	96~6
S8	5.70	0.1	0.12	0.05	5.6×10^5	96~6
S9	5.97	0.1	0.12	0.05	5.9×10^5	96~6
S10	6.24	0.1	0.12	0.05	6.1×10^5	96~6
S11	5.69	0.05	0.12	0.05	2.0×10^5	96~6
S12	7.17	0.05	0.12	0.05	2.5×10^5	96~6
S13	8.32	0.05	0.12	0.05	2.9×10^5	96~6
S14	8.92	0.05	0.12	0.05	3.1×10^5	96~6
S15	3.89	0.08	0.12	0.05	2.7×10^5	96~6
S16	4.40	0.08	0.12	0.05	3.1×10^5	96~6
S17	4.71	0.08	0.12	0.05	3.3×10^5	96~6
S18	5.16	0.08	0.12	0.05	3.6×10^5	96~6
S19	6.40	0.08	0.12	0.05	4.5×10^5	96~6
S20	6.64	0.08	0.12	0.05	4.7×10^5	96~6
S21	2.81	0.12	0.12	0.05	3.6×10^5	96~6
S22	3.41	0.12	0.12	0.05	4.4×10^5	96~6
S23	3.78	0.12	0.12	0.05	4.9×10^5	96~6

3. Analysis of Experimental Data

3.1. Effect of Jet Length

L_{max} was optically detected as the distance between the jet takeoff point at $x = 0$ and the reattachment point C of the lower jet trajectory on the chute bottom. L_{max} was measured without considering the influence of the cavity backwater, as shown in Figure 1. The L was an important factor in the evaluation of the cavity state. During the aeration process, a longer cavity was conducive to the addition of more air into the water. A longer bottom cavity increased the contact area between the lower surface of the jet and air, and the amount of air added along with the jet increased. To study the influence of atmospheric pressure on L_{max}, experiments at various atmospheric pressures were conducted according to the experimental conditions discussed above. The changes in L_{max} at different atmospheric pressures are presented in Figure 2a. The cavity subpressure was very small under all working conditions ($P_N < 0.1$). The data measurement results revealed that when $P_N < 0.1$, the influence of various atmospheric pressures on L_{max} was insignificant. The vacuum degree varied from 0 to 90%, and the value of L_{max} remained approximately constant with an error of less than 7.9%. This small measurement error was caused by fluctuations at the end of the bottom cavity and instability in the bottom cavity. L_{max} increased with an increase in F_0 when the approach flow depth was consistent, which was consistent with existing research results. Many studies have been conducted on jet length, and formulas for calculating jet length have been proposed with relatively high accuracy. Wu [16] established a calculation method for jet length considering the emergence angle and cavity subpressure according to the jet equation with high calculation accuracy. Pfister [19,20] considered that when the influence of cavity subpressure was ignored, $\Delta P \approx 0$ and the values of L_{max}/h were almost independent of the aeration concentration. The jet length was not affected by pre-aeration. According to the data analysis, L_{max} could be described explicitly in terms of the basic parameters instead of using the classical jet trajectory computation.

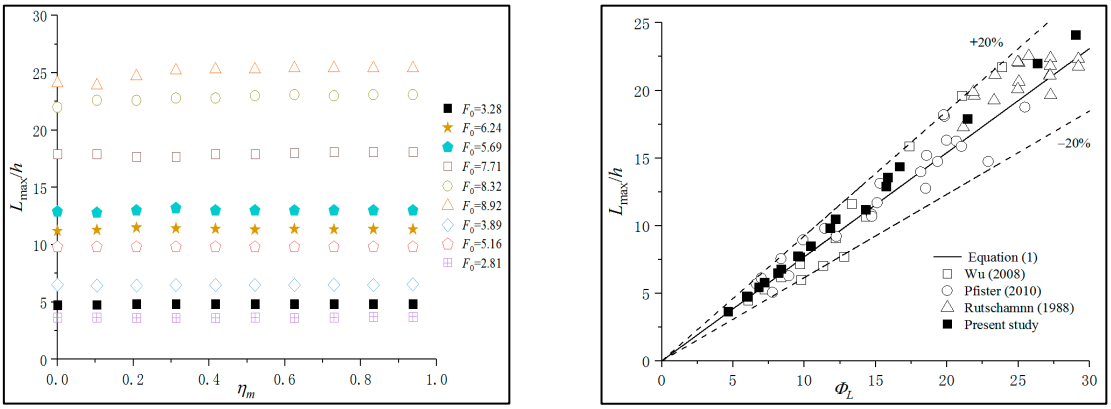

(**a**) (**b**)

Figure 2. The jet length. (**a**) Jet length at different atmospheric pressures; (**b**) the data compared with Equation (1).

L_{max} was a function of the downstream channel slope α, F_0, and the geometry of the aerator. When the bottom cavity pressure was approximately equal to the atmospheric pressure and there was no pre-aerated inflow condition, the maximum jet length was expressed as [21]:

$$\frac{L_{max}}{h} = 0.77F_0(1+\sin\alpha)^{1.5}\left(\sqrt{\frac{d}{h}} + F_0\tan\theta\right),\ \text{For}\ 0 < L/h < 50 \quad (1)$$

where θ is the emergence angle of the flow. Equation (1) can be used to approximately calculate the maximum jet length when the cavity subpressure is ignored. Only F_0, the aerator geometry, and the downstream channel slope affected the jet length. Figure 2b presents a comparison between the experimental data from Pfister, Wu, and Rutschmann, and the experimental measurements based on Equation (1), where $\Phi_L = F_0\ (1 + \sin\alpha)^{1.5}\ ((d/h)^{0.5} + F_0\tan\theta)$. For comparability, only a small cavity subpressure was considered in the experimental data ($P_N < 0.01$). Equation (1) describes the relationship between L_{max} and the aerator geometry, incoming flow conditions, and downstream channel slope.

The cavity subpressure was an important factor in determining L_{max}. L_{max} decreased with an increase in the cavity subpressure index P_N. Pfister [19] reported that the jet length decreased with an increase in P_N and that the cavity was typically blocked when $P_N > 1.0$. Therefore, a good ventilation environment is important for engineering applications. A reasonable ventilation size should be adopted to avoid large cavity subpressures and ensure uniform cavity airflow. When the small cavity subpressure can be ignored, meaning $\Delta P \approx 0$ and $P_N < 0.1$, it can be considered that the bottom cavity was well ventilated under these conditions. According to the experimental measurement results for the jet length, the cavity subpressure can be ignored when the air is fully ventilated. L_{max} was only a function of the approach flow conditions, aerator design parameters, and downstream channel slope. The data in Figure 2b were generated by using empirical Equation (1) to calculate L_{max} and contained relatively large errors. The errors of some data were greater than 20%. Comparatively, the method using jet theory to calculate the jet length was more accurate and widely used.

3.2. Effect of ΔP

ΔP is an important parameter for determining the characteristics of the bottom cavity [22,23]. ΔP affects the backwater of the bottom cavity, jet length, and air intake in the bottom cavity. In the tests, $P_N < 0.1$ and the influence of ΔP on the maximum jet length could be ignored. Changes in ΔP affected the air intake of the bottom cavity and cavity backwater. The test results revealed that the increase in air intake in the bottom cavity with an increase in ΔP for a given shaft size was constant. Under the same conditions, a

greater ΔP resulted in more significant backwater in the bottom cavity. The measurement results for ΔP are presented in Figure 3a. The measurement results for ΔP indicated that under the same conditions, the atmospheric pressure decreased with a decrease in ΔP. At normal atmospheric pressure ($\eta_m = 0$), ΔP reached its maximum value. With a decrease in atmospheric pressure, the pressure in the bottom cavity gradually approached atmospheric pressure. When $\eta_m = 1$, the water flowed in a vacuum, and $\Delta P = 0$. Under various atmospheric pressures, ΔP increased with an increase in F_0. This was consistent with the effects of F_0 on ΔP at atmospheric pressure. In Figure 3a, one can see that with a decrease in atmospheric pressure, the rate of decrease in ΔP was different for different approach flow conditions. The greater the value of F_0 is, the more rapidly ΔP decreases. From Conditions S2 and S4, ΔP was small at normal atmospheric pressure, and the atmospheric pressure changed by 30%, which caused ΔP to approach zero, where the bottom cavity pressure was equal to the atmospheric pressure. According to the measured ΔP data, the empirical Equation (2) was fitted to calculate ΔP at different atmospheric pressures, with $R^2 = 0.84$.

$$\Delta P = (-2.7F_0 - 27)\eta_m + \Delta P_a,\ 2.81 < F_0 < 8.92 \quad (2)$$

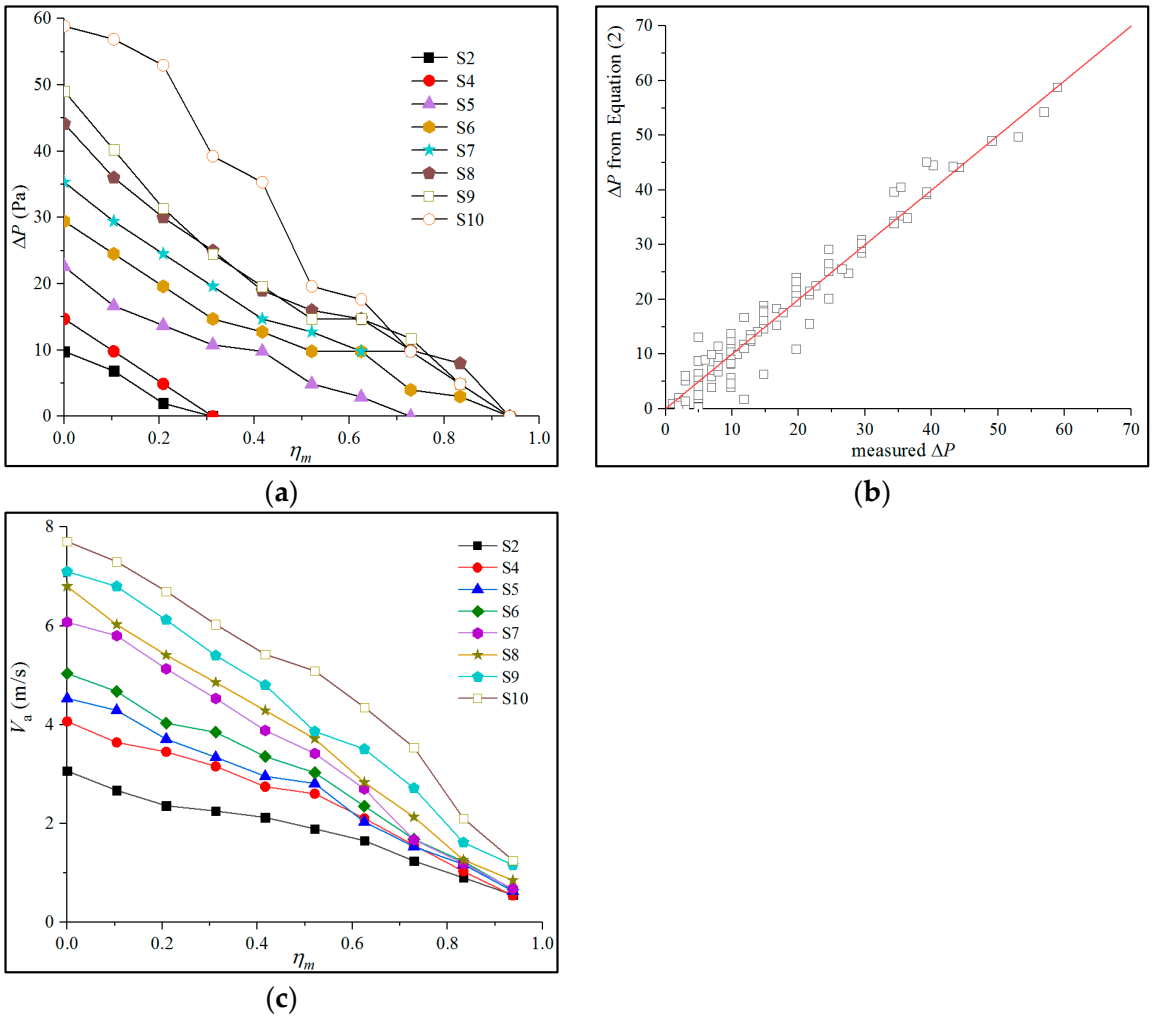

Figure 3. ΔP and air velocity at different atmospheric pressures. (**a**) Changes in ΔP; (**b**) ΔP computed by using Equation (2); (**c**) air velocity in the shaft.

In Equation (2), ΔP represents the cavity subpressure at different atmospheric pressures, and ΔP_a represents the cavity subpressure at normal atmospheric pressure. The relationship between cavity subpressure and atmospheric pressure is linear. The present tests indicated good agreement with Equation (2), as shown in Figure 3b.

Additionally, ΔP reflected the volume of air intake in the bottom cavity. When the size of the shaft was determined under the same conditions, the volume of air intake increased with an increase in ΔP. The volume of air intake determined the air velocity in the shaft, such that the greater the volume of the air intake was, the greater the air velocity in the shaft. The variation in air velocity in the shaft under various working conditions was measured in the tests. As shown in Figure 3c, the variation trend of the air velocity gradually decreased with a decrease in atmospheric pressure. Under the same conditions, the air velocity decreased with a decrease in F_0. ΔP affected the air intake in the bottom cavity. The smaller the value of ΔP, the smaller the air velocity and the lower the volume of air intake. It should be noted that the lower the atmospheric pressure was, the greater the error in the measured air velocity data. Airflow monitoring was not a professional instrument for measuring the air velocity in a low-pressure environment, and with an increase in η_{m}, the accuracy of the air velocity data in the shaft decreased. By comparing Figure 3a,c, the measured results for ΔP and the air velocity in the shaft can confirm each other. With a decrease in atmospheric pressure, the change laws of ΔP and the air velocity were consistent.

3.3. Effect of Backwater

A clear bottom cavity favored aeration. In engineering, backwater often occurs in the bottom cavity as a result of design defects in the aerator. When it was severe, backwater blocked the air inlet and closed the bottom cavity, making it difficult to introduce air into the water. Under normal atmospheric pressure (P_0 = 96 kPa), there were many factors affecting the backwater, including F_0, ΔP, and the shape parameters of the aerator. On the premise of ignoring changes in atmospheric pressure, it was considered that atmospheric pressure was not a parameter affecting backwater. Yang and Xu [9,10] presented a beneficial discussion on the problem of cavity backwater with P_0 = 96 kPa and established a calculation formula for cavity backwater at a low Froude number according to momentum balance. Although the influence of ΔP on backwater was considered in the formula, ΔP at a low Froude number was small. Therefore, ΔP was typically approximately zero in the calculation. Additionally, Pfister [11] discussed the influence of ΔP on backwater (0 kPa < ΔP < 4.9 kPa). The greater the value of ΔP, the greater the volume of backwater in the bottom cavity. However, there have been no research results regarding the influence of various atmospheric pressures on backwaters. Backwater data at different atmospheric pressures and low Froude numbers were measured in this experiment. Figure 4 presents the backwater under three conditions of a low Froude number. At P_a = 96 kPa, the backwater was the largest, and with a decrease in atmospheric pressure, the backwater decreased. At P_a = 6 kPa, the backwater was the lowest, and there was no observable backwater in the bottom cavity. Combined with the research results of ΔP, in the variation range of ΔP < 0.06 kPa, as the atmospheric pressure decreased from 96 kPa to 6 kPa, ΔP approached zero. Although the change range in ΔP was very small, the change in the backwater depth was very clear.

The backwater depths at different atmospheric pressures were measured during the tests, and the measurement results are presented in Figure 5a. The value of $y_0/y_{0(\mathrm{n})}$ represents the change in backwater depth with atmospheric pressure. $y_{0(\mathrm{n})}$ represents the backwater depth at P_0 = 96 kPa. The data indicated that the backwater depth decreased with a decrease in atmospheric pressure. When the atmospheric pressure was reduced by 90%, the backwater depth was reduced by at least 30% and at most 50%. For the same atmospheric pressure conditions, a change in the Froude number had the same influence on the backwater, and the backwater depth decreased with an increase in the Froude number. By comparing the backwater depth data for the same approach flow depth in Figure 5a, one can see that the gradient of the trend line of backwater depth increased with an increase in F_0 and that the backwater depth decreased faster with a decrease in atmospheric pressure. For example, for the approach flow depth h = 0.12 m, the atmospheric pressure decreased from 96 kPa to 6 kPa, and the backwater depth decreased by 29.5% in S21 and 50.9% in S3. The backwater depth affected the net length of the cavity. Under the same conditions, the

net length of the cavity decreased with an increase in backwater depth. The measurement results for the net length of the cavity are presented in Figure 5b. L_{net}/L_{max} represents the severity of backwater in the bottom cavity. $L_{net}/L_{max} = 0$ indicated that the bottom cavity was completely blocked by backwater. $L_{net}/L_{max} = 1$ indicated that there was no backwater in the bottom cavity. An increase in L_{net}/L_{max} indicated a decrease in backwater and a better shape of the bottom cavity. From the data in Figure 5, one can see that the changing trend of L_{net} was opposite to that of backwater depth. When the other conditions were constant, the value of L_{net} increased with a decrease in atmospheric pressure. The longer net length of the cavity caused the backwater to move away from the air inlet, which was conducive to the air intake in the bottom cavity. Figure 5b presents the influence of F_0 on L_{net}. Under the same conditions, the value of L_{net} increased with an increase in F_0. In the tests, the slope of the channel was slow, the water surface of the backwater in the bottom cavity was unstable, and the measurement results for the net length of the cavity contained measurement errors.

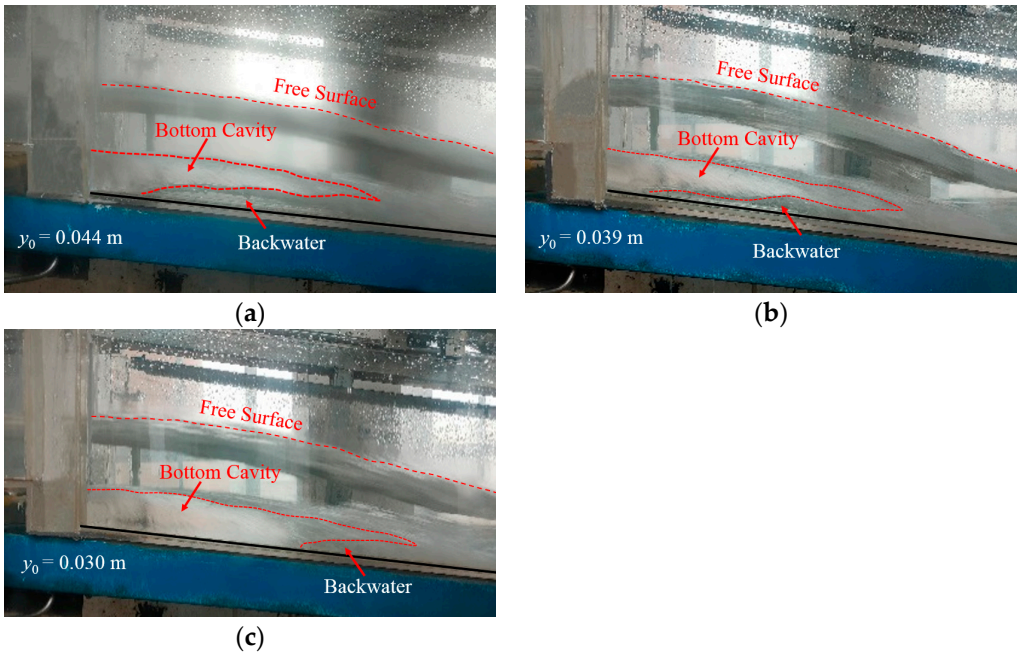

Figure 4. The backwater at different atmospheric pressure. (**a**) P_a = 96 kPa; (**b**) P_a = 56 kPa; (**c**) P_a = 6 kPa.

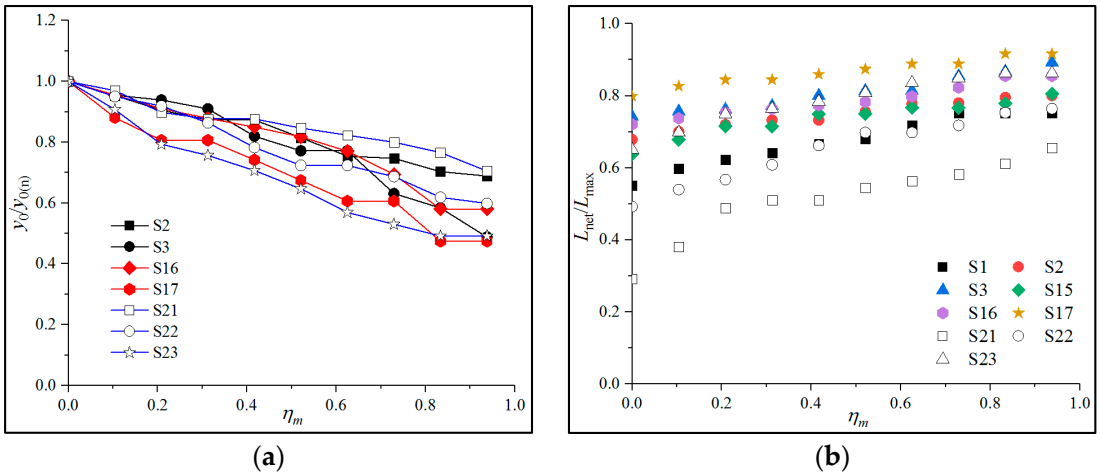

Figure 5. The backwater depth and L_{net} at different atmospheric pressures. (**a**) the change in backwater depth with η_m; (**b**) the relation between L_{net}/L_{max} and η_m.

4. Discussion

It is observed that a reduction in atmospheric pressure reduced ΔP in the model test, which led to the weakening of the cavity backwater. When $P_N < 0.1$, the influence of ΔP on jet length can be ignored. When the approach flow was constant, the flow velocity and jet length remained constant at different atmospheric pressures. ΔP decreased with a decrease in atmospheric pressure, and the cavity backwater weakened. At $P_0 = 96$ kPa, a defective air inlet led to insufficient air intake in the cavity, which increased ΔP and eventually increased the backwater depth. According to the test results, when the size of the air inlet was constant and the air demand was sufficient, a reduction in atmospheric pressure reduced ΔP, leading to the weakening of the cavity backwater. Yang and Xu [17,18] discussed changes in the backwater in the bottom cavity and established a calculation formula for backwater depth using the momentum equation, and the influence of ΔP on backwater was considered in their formula. Xu established a theoretical formula for cavity backwater at normal atmospheric pressure according to momentum balance. When ventilation was met, $\Delta P = 0$, and the momentum equations along the x-axis were [18]

$$k_1 y^2 + k_2 y + k_3 = 0 \tag{3}$$

$$k_1 = \frac{1}{2}\rho g \frac{\sin(\alpha + \theta_2)}{\sin\theta_2} \tag{4}$$

$$k_2 = \frac{1}{2}\rho g h \frac{\sin\alpha}{\sin\theta_2}(\cos(\alpha + \theta_1) + \cos(\alpha + \theta_2)) - \frac{\rho g h}{4}\frac{\sin 2(\alpha + \theta_2)}{\tan\theta_2} \tag{5}$$

$$k_3 = -\rho q v\left(\frac{\cos\theta_2}{\cos(\alpha + \theta_2)} - \frac{\cos\theta_1}{\cos(\alpha + \theta_1)}\right) \tag{6}$$

Equation (3) was used to calculate the backwater depth at normal atmospheric pressure ($P_0 = 96$ kPa), and the calculated results were compared with the experimental measurement results, as shown in Figure 6a. The calculated y_0 was slightly less than the measured value when $P_0 = 96$ kPa. However, y_0 decreased with a decrease in atmospheric pressure, and the difference between the experimental measurements and the calculated values increased. When the atmospheric pressure decreased from 96 to 16 kPa, y_0 was clearly less than the value calculated using Equation (3). According to the measurement results for y_0 in this study (Figure 5a), when the atmospheric pressure was reduced, there was still a significant change in the backwater, although there was only a small change in ΔP. Additionally, when combined with the results in Figure 3a, $\eta_m < 0.4$ and $\Delta P \approx 0$. The cavity backwater decreased with a decrease in atmospheric pressure. When η_m changed from 0 to 0.9, P_N changed by less than 0.02, and y_0 decreased by at most 50% and at least 30%. Equation (3) cannot calculate the backwater depth at low atmospheric pressures. Therefore, it was necessary to revise the formula for calculating the backwater depth proposed by Yang and Xu [17,18]. A decrease in atmospheric pressure reduced the cavity backwater or even eliminated it completely. Atmospheric pressure should also be considered as a parameter that affects cavity backwater.

According to the measured data, the backwater depth can be clearly expressed by the basic parameters instead of using the complex momentum balance equation calculation formula. For the dimensionless backwater depth, y_0/d was used for analysis. The value of y_0/d represents the change in backwater depth. The greater the value of y_0/d, the greater the backwater depth. For a lower F_0, the jet cavity was shorter, and the jet impinged on the bottom plate at a relatively steep angle, resulting in a larger offset and more water remaining in the cavity. The influence of the channel slope on the backwater depth was expressed as $(1 + \sin\alpha)$. The variables d and F_0 combined with h and described in the form of $1 + (d/(F_0\ h))^{0.5}$ represented the influence of the emergence angle on the backwater depth. The value of $(1 + \eta_m)^{0.5}$ was used to describe the influence of atmospheric pressure

on the backwater depth. Additionally, $(1 + P_N)$ represents the influence of ΔP on backwater depth. All parameters were combined to form the following offset function:

$$T = F_0\sqrt{(1+\eta_m)}\left(\frac{1+\sin\alpha}{1+P_N}\right)\left(1+\sqrt{\frac{d}{F_0 h}}\right),\ \text{for } 2.81 < F_0 < 4.76 \tag{7}$$

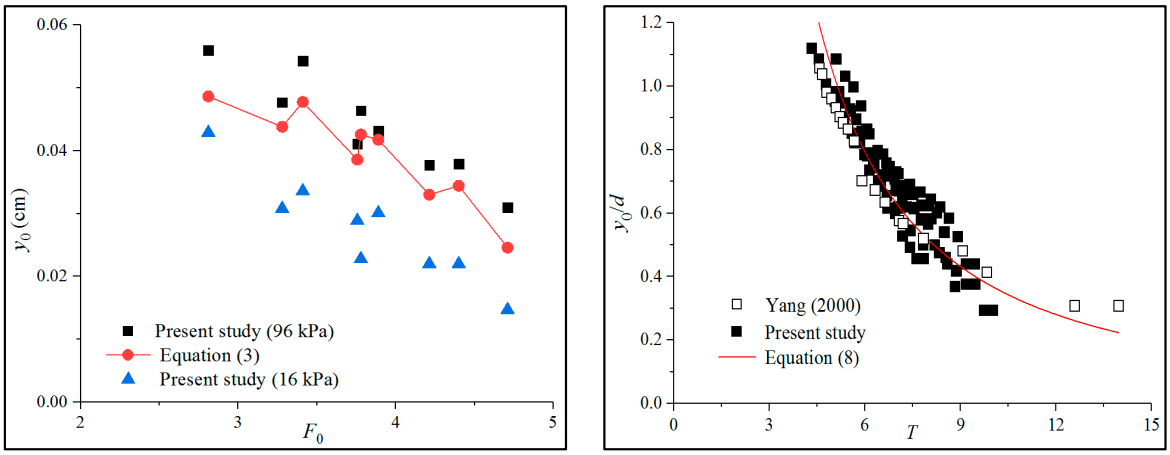

(a) **(b)**

Figure 6. Measurement and calculation data of y_0. (**a**) Experimental and calculated values of backwater depth; (**b**) comparison between Equation (8) with experimental data.

Figure 6b presents the relationship between T and y_0/d, indicating good agreement. The y_0/d trend was decreased. The trend of y_0/d may be expressed as an exponential function $y_0/d = 11.66\ (T^{-1.5})$, where $R^2 = 0.87$, as follows:

$$\frac{y_0}{d} = \frac{11.66}{\left[F_0\sqrt{(1+\eta_m)}\left(\frac{1+\sin\alpha}{1+P_N}\right)\left(1+\sqrt{\frac{d}{F_0 h}}\right)\right]^{1.5}} \tag{8}$$

P_N at different atmospheric pressures can be estimated using Equation (2). Equation (8) reflected the relationship between y_0, F_0, η_m, the aerator shape parameters, and α. According to the results of the study, a reduction in atmospheric pressure will inhibit backwater generation in the bottom cavity. The influence of the above parameters on the cavity backwater was consistent with the results reported in the literature and the data collected in the study. The experimental results demonstrated that the cavity backwater was less likely to block the air inlet at high altitudes when the other conditions were the same. Additionally, the amount of basic data used for fitting Equation (8) was relatively small, and this fitting requires further improvement. When ΔP varies over a larger range, it should be determined whether the change in the cavity backwater conforms to the trend in Equation (8). Varying the atmospheric pressure influenced ΔP, the net length of the cavity, and the volume of air intake. These parameters were related to aeration. Therefore, it was important to study the effects of atmospheric pressure on aeration. This was of great significance for the operational safety of flood discharge and aeration facilities in high-altitude areas.

According to the measurement results for ΔP and air velocity in the shaft at different atmospheric pressures (Figure 3), the air intake in the bottom cavity decreased with a decrease in atmospheric pressure under the same conditions. The air intake of the bottom cavity affected the air entrainment performance. A decrease in air intake led to a decrease in water flow aeration. The measurement results for backwater depth at a low Froude number indicated that a decrease in atmospheric pressure was beneficial for inhibiting backwater. Currently, the manner in which the backwater in the bottom cavity is understood under normal atmospheric pressure is that the weakening of the backwater benefits the air intake and that the weakening of the backwater can increase the net length of the cavity. A larger

bottom cavity was beneficial to the air intake and air entrainment. However, according to the test results, with a decrease in atmospheric pressure, the cavity backwater weakened, and the air intake decreased. When the atmospheric pressure decreased, the influence of the reduction in backwater on air intake became less significant. In contrast, the influence of atmospheric pressure on air intake became more prominent.

5. Conclusions

The hydraulic model test introduced in this paper allowed us to complete basic research on cavity backwater at different atmospheric pressures. In the framework of this basic investigation, the relevant parameters, atmospheric pressure, Froude number, and other factors were systematically varied. The cavity subpressure, backwater depth in the cavity, jet length, and air velocity in the shaft were measured. The study of backwater at different atmospheric pressures yielded the following conclusions.

Varying the atmospheric pressure affected the cavity subpressure. With a decrease in atmospheric pressure, the cavity subpressure decreased and eventually approached zero, meaning the pressure in the cavity became equal to the atmospheric pressure. For a well-ventilated bottom cavity with $P_N < 0.1$, the cavity subpressure could be ignored, and the influence of atmospheric pressure on the maximum jet length could be ignored. Additionally, a decrease in atmospheric pressure reduced the air velocity in the shaft, and it was determined that a decrease in atmospheric pressure led to a decrease in the air intake.

At low atmospheric pressures, it was more difficult to produce cavity backwater, significantly reducing the risk of backwater clogging the inlet hole. Additionally, a decrease in the backwater increased the net length of the cavity, so the net length of the cavity increased with a decrease in atmospheric pressure. Furthermore, an improved equation was proposed to calculate the backwater depth. The vacuum degree of the tests varied from 0 to 0.9. In the study, the shape of the aerator was considered as the aerator step, and the effects of the emergence angle on the cavity backwater were not considered. It was suggested that the aerator and air supply system should be optimized to reduce energy loss in the shaft. The results of the study have guiding significance for the design and construction of spillways and aeration facilities in high-altitude areas. This paper focused on the effect of the pressure difference between inside and outside the cavity caused by atmospheric pressure on backwater. The influence of atmospheric pressure on the water phase and gas phase in the water body and the change of Euler number of water flow will lead to the difference of water-air two-phase flow characteristics under low atmospheric pressure compared with normal atmospheric pressure. It needs targeted research in future model tests.

Author Contributions: Y.W. made hydraulic model, data collection and manuscript writing. W.W. analyzed preliminary results and revised the manuscript. J.D. was responsible for funding acquisition, supervision of physical modeling and revision of the manuscript. All authors have read and agreed to the published version of the manuscript.

Funding: This research was funded by [the National Natural Science Foundation of China] grant number [51939007, 51979182] and [the Sichuan Science and Technology Program] grant number [2019JDTD0007].

Conflicts of Interest: The authors declare no conflict of interest.

Abbreviations

The following symbols were used in this paper:

P_0	normal atmospheric pressure (kPa)
P_a	atmospheric pressure inside the pressure-reducing tank (kPa)
ΔP	cavity subpressure (Pa)
P_c	cavity pressure (kPa)
P_N	cavity subpressure index (−)
ΔP_a	cavity subpressure under normal atmospheric pressure (Pa)
V_0	approach flow velocity (m/s)
L_{max}	maximum jet length (m)
L_{net}	net length of the cavity (m)
F_0	Froude number (−)
Re	Reynolds number (−)
d	aerator height (m)
g	gravitational acceleration (m/s^2)
h	approach flow depth (m)
h_s	cavity subpressure head (m)
i	downstream chute slope (−)
q	unit width flow (m^3/s)
y_0	depth of backwater (m)
α	downstream chute angle (°)
ρ	density of water (kg/m^3)
θ	deflector angle of water (°)
θ_1	the included angle between the jet trajectory and x-axis at the top point of the backwater (°)
θ_2	the included angle between the end trajectory of jet flow and the x-axis (°)
v	kinematic water viscosity (m^2/s)
η_m	vacuum degree (−)

References

1. Koschitzky, H.-P. *Dimensionierungskonzept für sohlbelüfter in schussrinnen zur vermeidung von kavitationsschäden [Design Concept for Chute Aerators to Avoid Cavitation Damage]*; Mitteilung, 65; Institut für Wasserbau, TU Stuttgart: Stuttgart, Germany, 1987. (In German)
2. Rutschmann, P. *Belüftungseinbauten in schussrinnen [Chute Additions for Air Entrainment]*; Mitteilung, 97; Vischer, D., Ed.; Laboratory of Hydraulics, Hydrology and Glaciology (VAW), ETH: Zurich, Switzerland, 1988. (In German)
3. Chanson, H. Study of Air Entrainment and Aeration Devices on Spillway Model. Ph.D. Thesis, University of Canterbury, Christchurch, New Zealand, 1988.
4. Skripalle, J. *Zwangsbelüftung von hochgeschwindigkeits strömungen an zurückspringenden stufen im wasserbau [Forced Aeration of High-Speed Flows at Chute Aerators]*; Mitteilung, 124; Technische Universität: Berlin, Germany, 1994. (In German)
5. Khatsuria, R.M. *Hydraulics of Spillways and Energy Dissipators*; CRC Press: New York, NY, USA, 2004.
6. Vischer, D.L.; Hager, W.H. *Dam Hydraulics*; John Wiley & Sons: Chichester, UK, 1998.
7. Chanson, H. Study of air entrainment and aeration devices. *J. Hydraul. Res.* **1989**, *27*, 301–319. [CrossRef]
8. Kokpinar, M.A.; Gogus, M. High-speed jet flows over spillway aerators. *Can. J. Civ. Eng.* **2002**, *29*, 885–898. [CrossRef]
9. Bhosekar, V.V.; Jothiprakash, V.; Deolalikar, P.B. Orifice spillway aerator: Hydraulic design. *J. Hydraul. Eng.* **2012**, *138*, 563–572. [CrossRef]
10. Kramer, K. Development of Aerated Chute Flow. Ph.D. Thesis, Laboratory of Hydraulics, Hydrology and Glaciology (VAW), ETH, Zurich, Switzerland, 2004.
11. Pan, S.B.; Shao, Y.Y.; Shi, Q.S. The self-aeration capacity of the water jet over the aeration ramp. *J. Hydraul. Eng. ASCE* **1980**, *5*, 13–22. (In Chinese)
12. Rutschmann, P.; Hager, W.H. Air entrainment by spillway aerators. *J. Hydraul. Eng. ASCE* **1990**, *116*, 765–782. [CrossRef]
13. Rutschmann, P.; Hager, W.H. Design and performance of spillway chute aerators. *Int. Water Power Dam. Constr.* **1990**, *42*, 36–42.
14. Shi, Q.S.; Pan, S.B.; Shao, Y.Y. Experimental investigation of flow aeration to prevent cavitation erosion by a deflector. *J. Hydraul. Eng.* **1983**, *3*, 1–13. (In Chinese)
15. Wei, C.Y.; Defazio, F.G. Simulation of free jet trajectories for the design of aeration devices on hydraulic structures. In *Finite Elements in Water Resources, Proceedings of the the 4th International Conference, Hannover, Germany, June 1982*; Springer: Berlin/Heidelberg, Germany, 1982; pp. 1745–1755.
16. Wu, J.; Ruan, S. Cavity length below chute aerators. *Sci. China Ser. E-Technol. Sci.* **1983**, *51*, 170–178. [CrossRef]

17. Yang, Y.; Yang, Y. The hydraulic and aeration characteristics of low froude number flow over a step aerator. *J. Hydraul. Eng.* **2000**, *2*, 27–31.
18. Xu, Y.; Wang, W.; Yong, H.; Zhao, W. Investigation on the cavity backwater of the jet flow from the chute aerators. *Procedia Eng.* **2012**, *31*, 51–56. [CrossRef]
19. Pfister, M. Chute aerators: Steep deflectors and cavity subpressure. *J. Hydraul. Eng.* **2011**, *137*, 1208–1215. [CrossRef]
20. Pfister, M.; Hager, W.H. Chute aerators I: Air transport characteristics. *J. Hydraul. Eng.* **2010**, *136*, 352–359. [CrossRef]
21. Pfister, M. Schussrinnenbelüfter: Lufttransport Ausgelöst durch Interne Abflussstruktur [Chute Aerators: Air Transport due to Internal Flow Structure]. Ph.D. Thesis, Laboratory of Hydraulics, Hydrology and Glaciology (VAW), ETH, Zurich, Switzerland, 2008. (In German)
22. Yang, J.; Lin, C.; Kao, M.J.; Teng, P.; Raikar, R.V. Application of SIM, HSPIV, BTM, and BIV techniques for evaluations of a two-phase air-water chute aerator flow. *Water* **2018**, *10*, 1590. [CrossRef]
23. Yang, J.; Teng, P.; Xie, Q.; Li, S. Understanding water flows and air venting features of spillway-A case study. *Water* **2020**, *12*, 2106. [CrossRef]